Proceeding of the IEEE
International Conference on Robotics and Biomimetics
Dali, China, December 2019

A Multibeam Underwater Terrain Modeling Algorithm Based on Echo Energy Distribution Gradient*

Yipeng Tang
Key Laboratory of Measurement and Control of Complex Systems of Engineering (School of Automation)
Southeast University
Nanjing, Jiangsu Province 210096, China
220171511@seu.edu.cn

Bo Zhou
Key Laboratory of Measurement and Control of Complex Systems of Engineering (School of Automation)
Southeast University
Nanjing, Jiangsu Province 210096, China
zhoubo@seu.edu.cn

***Abstract* –In the field of underwater robot, abundant researches have been carried out in development of multibeam echo-sounding bottom detection. However, most works focused on the analysis of the amplitude of the reverberated echo which had its own limitation. In this paper, a new algorithm based on the multibeam echo energy gradient is developed to map the shallow water bottom topography. On this basis, all single-frame bottom depth curves are joined together to form a seabed surface. Kalman filter is further used to remove outliers and improve the reliability of surface mapping. The effectiveness of our algorithm is validated by both simulation and practical experiment.**

Index Terms - Underwater robot; Multibeam echo; Underwater mapping; Energy gradient

I. INTRODUCTION

With the development of ocean, the research of underwater vehicle technology has become a hot research topic. At present, underwater robots are widely applied in underwater pipeline inspection, ship repair, underwater entertainment, underwater archaeology, scientific research, etc. [1] Among these applications, underwater terrain modeling is an important part because detecting and visualizing underwater terrain is the basis of underwater robot navigation and operation. Furthermore, it provides valuable underwater environment data for further studies. Therefore, it is necessary to develop a reliable and effective underwater terrain modeling method to enhance the accuracy.

In recent years, many algorithms conducting underwater terrain modeling are based on acoustic methods. In particular, the echo-integration is a common technique for estimating terrain and it can be divided into two categories, namely the single- and multi- beam echo-sounding. Traditional single-beam echo-sounding can sample the water column inside a sphere, whose radius is the bottom depth, when there is no interference from the bottom reverberation [2]. Multibeam echo-sounding, as a new generation of system, has superseded the single-beam method and has been employed to conduct sea-floor mapping for about 20 years [3]. This new system is able to cover the whole angle range and can provide acoustic images comparable to those obtained by side-scan sonars.

There are three mainstreams in bottom detection techniques based on multibeam echo-sounding: (1) a weighted mean time of arrival is estimated for each beam [4], (2) angles of arrival are estimated for each time increment through a beam deviation indicator algorithm [5], or (3) echo arrival time-angle pairs are derived from the zero crossing of phase in a split aperture correlator [6]. The bottom-detection algorithms implemented in most real echosounders are amplitude detectors.

In this paper, we improve Lurton`s processing scheme [7], which belongs to the first bottom detecting mainstream. In this method, the X coordinate of the peak signal is taken as the depth of the bottom. Further, to obtain robustness, they implement the average X coordinate of two samples whose amplitude is less than the peak for more than 10dB to approximate that of the peak signal. However, the maximum-amplitude method cannot cope with the situation where the incidence of echo is larger than 20°, because under this circumstance, the front edge of echo amplitude is not steep enough, degrading the accuracy of detection [8]. In addition, the side-lobe effect, which is caused by the energy leakage of the emitter array located at the long interference point, confuses the main lobe echo, leading to the misdetection and detection deviation.

To this end, a multibeam bathymetric algorithm based on echo energy gradient is proposed to extract the real bottom position directly from the amplitude distribution of multibeam echosounders. To validate the effectiveness of our method, we conduct extensive experiments on both practical and simulated data. The practical data are collected by a Reson SeaBat7125 multibeam sonar equipped with moored underwater acoustic transponders and contains numerous interference signals, which would pose challenges to any bottom detection algorithm. The simulation data, meanwhile, is obtained by MATLAB.

This paper is organized as follows. Section Ⅱ describes the processing steps applied to each amplitude signal in a ping and section Ⅲ presents a method which is applied in a continuous sequence of pings. To validate the proposed algorithm, simulations and real data processing are shown in section Ⅳ while section Ⅴ presents the conclusion.

* Research supported by National Natural Science Foundation (NNSF) of China under Grant 61573100, 61573101, 61673254 and U1613226.

978-1-7281-6321-5/19//$31.00 ©2019 IEEE

Ⅱ. IMPROVING AMPLITUDE-BASED DETECTION

A. Analysis of amplitude data

In the process of multi-beam sounding, the transducer equipped on the hull emits pulses which propagate to the object in the form of spherical waves. The backscatter to the transducer forms a frame of underwater acoustic data in the original path. Each frame of data contains a sequence of pixels reflecting the characteristics of seabed sediment and each pixel reflects its corresponding sound intensity. The original waterfall map can be obtained by stacking the collected echoes according to the order of measurement [9]. The decoded port and starboard echoes are processed separately, and each echo is arranged horizontally according to the sampling order to get a PING data. Then the PING data is applied in the measurement order and stacked vertically, so that the two-dimensional echo data matrix can be obtained. The multi-beam bathymetry diagram is shown in Fig. 1.

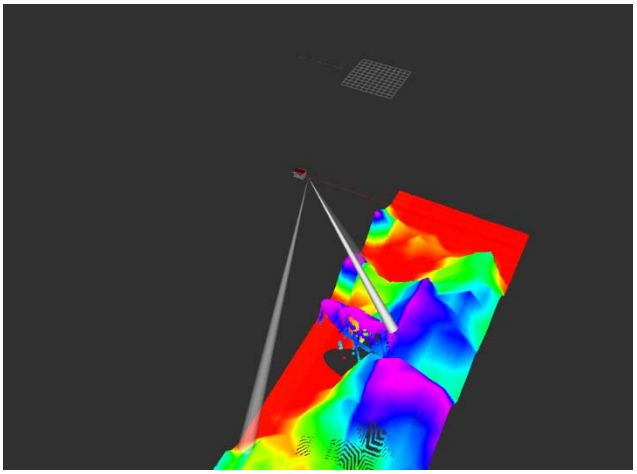

Fig. 1 Multi-beam bathymetry diagram

The echo matrix consists of three parts:(1) the reflection of the seabed, (2) disturbance from random noise, (3) side lobe interference.

Due to the sidelobe effect of multi-beam transducer, there exist two types of sidelobe interference in water data, i.e. the receiving sidelobe interference and the transmitting sidelobe interference. Sound wave irradiates the seabed area of edge beam with small grazing angle. The echo propagation range in this area is more extensive and the propagation loss is larger, which results in smaller amplitude and wider spread of echo signal. This phenomenon is called receiving sidelobe interference [10]. The transmitting sidelobe interference, meanwhile, is most obvious one when detecting inclined terrain and strong reflection seabed. The echo of such sidelobe is usually delayed by the main lobe and is recorded by the next Ping because of its oblique projection to the seabed [11].

As shown in Fig. 2, the transmitting sidelobe interference is the most conspicuous one. The area contained in black box indicate the echo of the real bottom and that caused by the sidelobe interference respectively. It is apparent that calculating the exact location information of this area is difficult.

There are also ship noise interference and signal interference caused by other acoustic detection equipment on board [12]. These types of interference have the same or even stronger effect as the emission sidelobe interference, resulting in difficulties in estimating the depth of water. Generally, the distribution of these interferences is irregular, and they may exist in any part of the water body data. Fortunately, their energy is relatively small and barely affects the interpretation of water body data, therefore can be omitted when processing the amplitude data.

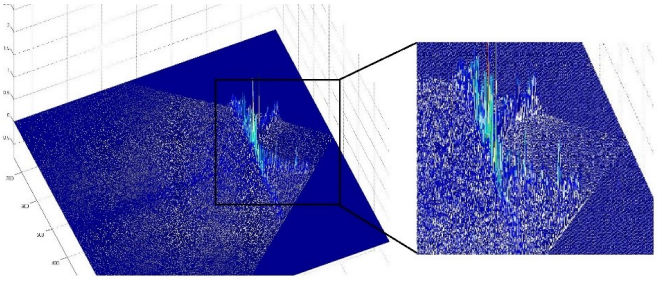

Fig. 2 Echo amplitude curve affected by sidelobe effect

As shown in Fig. 3, when the incident angle is larger, the detection is unsatisfactory because the front edge of the echo amplitude is not steep enough to provide accurate seabed detection.

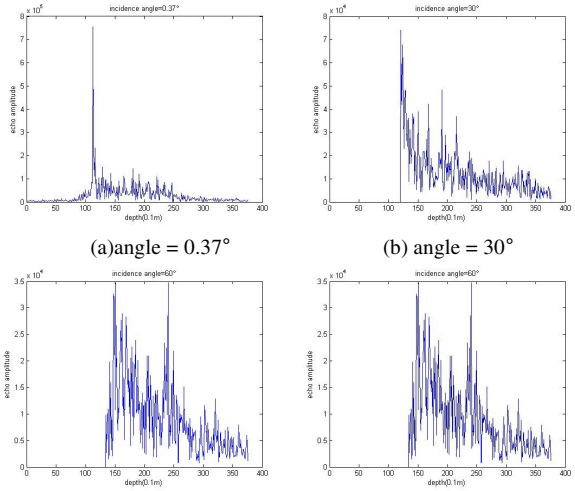

(a)angle = 0.37° (b) angle = 30°

(c)angle = 45° (d) angle = 60°

Fig. 3 Echo amplitude of different incident angle

B. Algorithm of Bottom detection based on energy gradient

In this section, we propose an underwater location detection algorithm based on energy gradient of the echo amplitude. The noise interference is minimized, on the basis of the characteristics of the energy distribution of echo, to extract the underwater echo region.

For grey images ranging in [0,255], the grey level histogram is a one-dimensional discrete function, expressed as (1):

$$p(g_i)=\frac{n_i}{n}(i=0,1,2\cdots\cdots,255) \tag{1}$$

where g_i is the i-th grey value of the grey image $f(x,y)$, n_i is the number of pixels with grey value g_i in $f(x,y)$, n is the total number of pixels in image $f(x,y)$, $P(g_i)$ is the probability estimation of the occurrence of the first grey value.

Energy E_{energy} of the image can be represented as (2):

$$E_{energy}=\sum_{i=0}^{255}P(g_i)^2 \tag{2}$$

The energy $E_{energy}(x,y)$ of each pixel $f(x,y)$ in grey image can be calculated and forms a new energy matrix E as (3):

$$E=\begin{bmatrix} E_{energy}(x_1,y_1) & E_{energy}(x_1,y_2) & \cdots & E_{energy}(x_1,y_n) \\ E_{energy}(x_2,y_1) & E_{energy}(x_2,y_2) & \cdots & E_{energy}(x_2,y_n) \\ \vdots & \vdots & \ddots & \vdots \\ E_{energy}(x_n,y_1) & E_{energy}(x_n,y_2) & \cdots & E_{energy}(x_n,y_n) \end{bmatrix} \tag{3}$$

Then the horizontal and vertical gradients (i.e. the gradients in x and y direction respectively of the new matrix E are computed. The horizontal gradient is obtained by convoluting the image with [1,0,-1] gradient operator, while the vertical gradient is calculated by convoluting the image with $[1,0,-1]^T$ operator. $G_x(x,y)$ and $G_y(x,y)$ represent the gradient of the image in the x-axis and y-axis directions at the pixel point (x,y), respectively, and $H(x,y)$ denotes the pixel value at that point. The size and direction of the gradient at the pixel point (x,y) are computed as follows (4),(5):

$$G(x,y)=\sqrt{G_x(x,y)^2+G_y(x,y)^2} \tag{4}$$

$$\alpha(x,y)=\tan^{-1}\left(\frac{G_y(x,y)}{G_x(x,y)}\right) \tag{5}$$

In this gradient image, the real seabed curve will show obvious boundary in the vertical direction, while the high grey area caused by sidelobe interference will be suppressed. The good results of bottom terrain can be obtained by extracting the processed image as (6):

$$C(x)=\max Index\left(Amp(x,:)\right) \tag{6}$$

where $C(x)$represents the x-th beam position on the bottom of the water. max*Index* is the function to get the location of the element with the largest amplitude in the numerical sequence. $Amp(x,:)$ is the amplitude curve of x-th beam.

The algorithm of bottom detection is given follow:

Step1: The echo amplitude data is converted into grey-scale images ranging in [0,255].

Step2: Calculate the energy of each pixel according to (1). And forms them as a new matrix E .

Step3: After get the horizontal and vertical gradients of the E, the gradient matrix $G(x,y)$ can be further obtained by (4).

Step4: The result of bottom curve can be detected (using (4) (5)).

Step5: To other PING data, we repeat Step 1 through Step 4.

Above can extract the curve of single PING data. The longitudinal coordinate value corresponding to each point of the curve is the depth value corresponding to that point.

Ⅲ. KALMAN-FILTERING ALGORITHM

In this section, the Bayesian estimation framework of bottom tracking is discussed. It relies on the definition of a likelihood function that describes the confidence in amplitude-based bottom detection. Considering the regularity of the bottom between two incident angles, a state-space, prior model is proposed. Using Kalman filtering, both information sources are merged and a robust estimate of the bottom location is computed.

A. Statistical description of bottom detection

For the sake of clarity, only single-beam data are considered here. Suppose that for ping k ,the true bottom location is at depth z_k and has been detected at depth y_k by the method in section Ⅱ. Then $y_k = z_k + e_k$, where the error e_k is unknow. Suppose that $\{e_k\}_k$ is a sequence of independent random variables, according to some probability distribution: $e_k \sim p_k(e_k)$ Then, the likelihood function is defined as (7):

$$L(y_k \mid z_k) \propto p_k(y_k - z_k) \tag{7}$$

With no additional knowledge of the error statistics, the Gaussian assumption as (8) is the most reasonable choice:

$$p_k(e_k)=g_\sigma(e_k)\equiv\frac{1}{\sigma\sqrt{2\pi}}\exp\left(-\frac{e_k^2}{2\sigma^2}\right) \tag{8}$$

The likelihood function is as (9):

$$\begin{aligned} L(y_k \mid z_k) &= \frac{1}{\sigma\sqrt{2\pi}}\exp\left(\frac{(y_k-z_k)^2}{2\sigma^2}\right) \\ &= \frac{1}{\sigma\sqrt{2\pi}}\exp\left(-\frac{e_k^2}{2\sigma^2}\right) \end{aligned} \tag{9}$$

It is considered that the distribution of deviation is Gauss distribution. But in practical application, in order to conform to the actual deviation as much as possible, a mixed distribution model with both mixed Gauss distribution and uniform distribution can be established as (10):

$$L(y_k \mid z_k)=\varepsilon U_\Delta(z_k)+(1-\varepsilon)\sum_{m=1}^{M}g_\sigma\left(z_k-y_k^{(m)}\right) \tag{10}$$

Where U_Δ denotes uniform distribution, $\Delta=[z_{\min},z_{\max}]$, ε is a mixed parameter which $\varepsilon\in[0,1]$, $y_k^{(m)}$ represents several depth values that meet the detection conditions in the ping k .

It can be obtained that:

$$\begin{aligned} L(y_k \mid z_k) &= \varepsilon U_\Delta(z_k)+(1-\varepsilon)\sum_{m=1}^{M}g_\sigma(z_k-y_k^{(m)}) \\ &= \varepsilon U_\Delta(z_k)+(1-\varepsilon)\sum_{m=1}^{M}\frac{1}{\sigma\sqrt{2\pi}}\exp(-\frac{(z_k-y_k^{(m)})^2}{2\sigma^2}) \\ &= \varepsilon U_\Delta(z_k)+\frac{1-\varepsilon}{\sigma\sqrt{2\pi}}\exp[-\frac{1}{2\sigma^2}\sum_{m=1}^{M}(z_k-y_k^{(m)})^2] \end{aligned} \tag{11}$$

B. Spatial regularity

Using the above notations, we introduce spatial regularity in expressing that z_k, the true bottom location at incidence angle k, should be close to that at incidence angle k-1. A

simple model is that the position of the water bottom can be regarded as a continues curve. As shown in Fig.4.

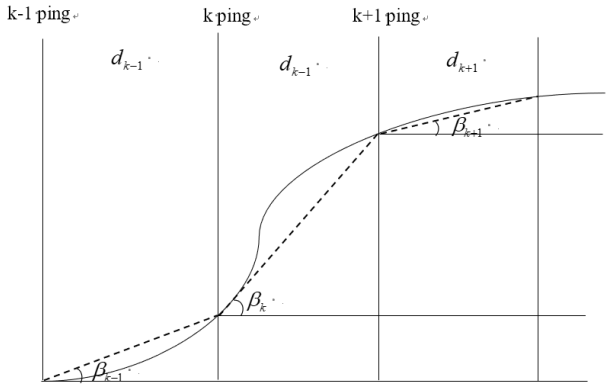

Fig. 4 Model of underwater bottom

A model takes a slope parameter into account as (12):

$$z_k = z_{k-1} + \dot{z}_{k-1}(z_k - z_{k-1}) + \ddot{z}_{k-1}\frac{(z_k - z_{k-1})^2}{2} + R_n(x) \tag{12}$$

Where $R_n(x)$ is remainder, $\dot{z}_{k-1}$ is the first derivative of bottom location which represents the trends of seabed curves, $\ddot{z}_{k-1}$ is the second derivative of bottom location.

In matrix form, the following linear model can be written as (13):

$$\begin{bmatrix} z_k \\ \dot{z}_k \\ \ddot{z}_k \end{bmatrix} = \begin{bmatrix} 1 & dx & \frac{dx^2}{2} \\ 0 & 1 & dx \\ 0 & 0 & 1 \end{bmatrix} \begin{bmatrix} z_{k-1} \\ \dot{z}_{k-1} \\ \ddot{z}_{k-1} \end{bmatrix} + \begin{bmatrix} v_{k-1}^{(z)} \\ v_{k-1}^{(a)} \\ v_{k-1}^{(g)} \end{bmatrix} \tag{13}$$
$$\Leftrightarrow X_k = F_{k-1}X_{k-1} + \gamma_{k-1}$$

Where d_{k-1} is the linear distance covered by the ship between the two incidence angles and γ_{k-1} represents the error made by linearly interpolating the bottom location at incident k from the bottom depth and slop at incident angle k-1

Model is a state-space prediction model that describes the spatial regularity of the seabed in the athwartship direction. Here γ_k is considered Gaussian, with zero mean and covariance:

$$Cov(\gamma_k) \equiv \sum_{\gamma} \equiv \begin{bmatrix} \mathrm{var}\,\gamma_{k-1}^{(z)} & 0 & 0 \\ 0 & \mathrm{var}\,\gamma_{k-1}^{(a)} & 0 \\ 0 & 0 & \mathrm{var}\,\gamma_{k-1}^{(g)} \end{bmatrix} = \begin{bmatrix} \sigma_z^2 & 0 & 0 \\ 0 & \sigma_a^2 & 0 \\ 0 & 0 & \sigma_g^2 \end{bmatrix} \tag{14}$$

With given variances σ_z^2 , σ_a^2 and σ_g^2 .Under this assumption, model can be presented as a probabilistic prediction term.

$$p(X_k \mid X_{k-1}) = \frac{1}{2\pi|\Sigma_r|}\exp\left(-\frac{1}{2}(X_k - F_k X_{k-1})' \sum_{\gamma}^{-1}(X_k - F_k X_{k-1})\right) \tag{15}$$

The state space model in multi-beam bathymetry can be clearly established as (16):

$$\begin{cases} X_k = F_{k-1}X_{k-1} + \Upsilon_{k-1} \\ Y_k = CX_k + V_k \end{cases} \tag{16}$$

C. Kalman filter

Until now, the statistical framework has been based on the definition of the likelihood function for bottom detection in incident angle and for every ping.

The Kalman filter consists of a time update and a measurement update. In the time update, the filter coefficients and their error covariances at time n are updated using only the measurements available until the previous time instant n-1. Such estimates are referred to as a priori estimates and are denoted using. The time update for is given by (17), (18):

$$\hat{x}_{\bar{k}} = A\hat{x}_{k-1} + Bu_{k-1} \tag{17}$$

$$\hat{x}_{\bar{k}} = A\hat{x}_{k-1} + Bu_{k-1} \tag{18}$$

as the measurement at time n become available, the parameter estimates and their error variance estimates are updated in the measurement update as follows (19), (20), (21):

$$K_k = \frac{P_{\bar{k}}H^T}{HP_{\bar{k}}H^T + R} \tag{19}$$

$$\hat{x}_k = \hat{x}_{\bar{k}} + K_k\left(z_k - H\hat{x}_{\bar{k}}\right) \tag{20}$$

$$P_k = \left(I - K_k H\right)P_{\bar{k}} \tag{21}$$

Where K_k is commonly referred to as Kalman gain and the error covariance P_k is defined by replacing $\hat{x}_{\bar{k}}$ with $\hat{x}_k$.

Ⅳ. TEST AND EXPERIMENT

A) Simulation environment

In this section, the simulation data of underwater terrain echo intensity data are simulated using Phased Array System Toolbox. The first echo intensity data of each frame is a matrix of 100*X*768, totalling 2297 frames, and the other data is totalling 5013 frames.

In order to quantitatively verify the bottom detection effect of this algorithm, this section uses MSE to evaluate the bottom detection results. MSE is usually used to evaluate the noise in the signal. The difference between the former and the latter is measured by calculating the MSE between the true value of the simulation data and the bottom detection results. The MSE formula is as (22):

$$MSE = \frac{1}{M}\sum_{M}[I_1(m) - I_2(m)]^2 \tag{22}$$

Where $I_1(m)$ is referred to as result of bottom detection. $I_2(m)$ is referred to as ground truth. M represents the beam sequence and m represents the beam sequence number.

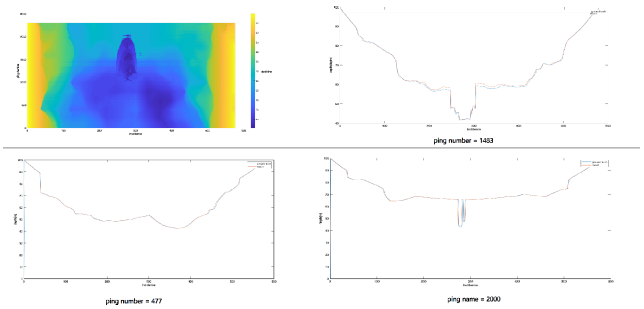

Fig. 5 Data set one and its bottom detection result display; when ping number = 1483, MSE= 1.9383, when ping number =477, MSE = 1.2486, when ping number = 2000, MSE = 1.5142.

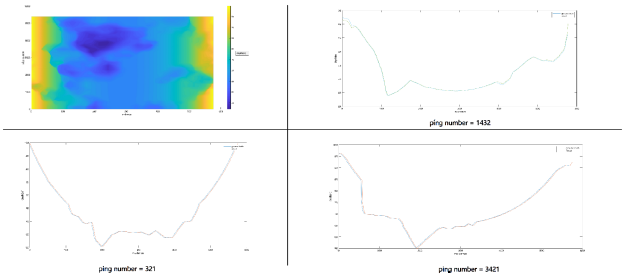

Fig. 6 Data set one and its bottom detection result display; when ping number = 1432, MSE= 1.7624, when ping number =321, MSE = 1.3425, when ping number = 3421, MSE = 1.2351

The comparison between the curve and the true value of the simulation data is shown in Fig.5 and Fig.6, and three frames of data are selected for display. The overall MSE results are shown in Table 1.

Table1 MSE results for two scenes

data	1	2
max MSE(*m*)	1.9383	1.7624
min MSE(*m*)	0.8424	0.6342
avg MSE(*m*)	1.4326	1.2135

From Table 1, we see that the proposed approach achieves high precision.

B) Real data of single beam

In order to test the effectiveness of the algorithm, two groups of multibeam data with serious sidelobe interference are selected for comparative experiment. Each group of data contains 751 beam sequences, of which 299 are valid sequences, that is, 299 depth values can be obtained. In this paper, the error detection rate is used as the evaluation index to evaluate the quality of sounding.

Bottom-detection result with amplitude-based method are illustrated in the Fig.7(a). It can be seen that sidelobe interference interferes with the detection results. In Fig.7(b), the algorithm based on echo energy gradient can remove the false terrain caused by sidelobe interference.

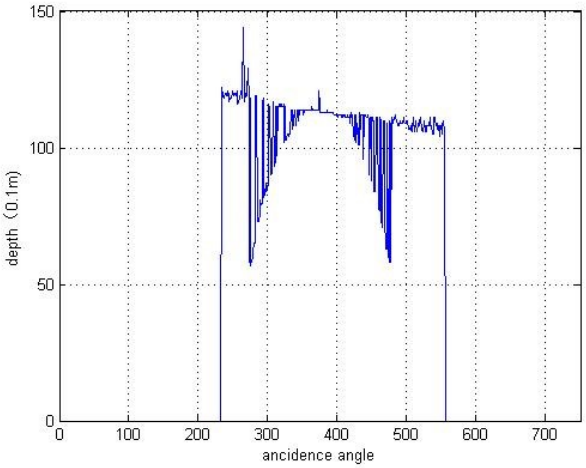

(a)Bottom-detection result with amplitude-based method

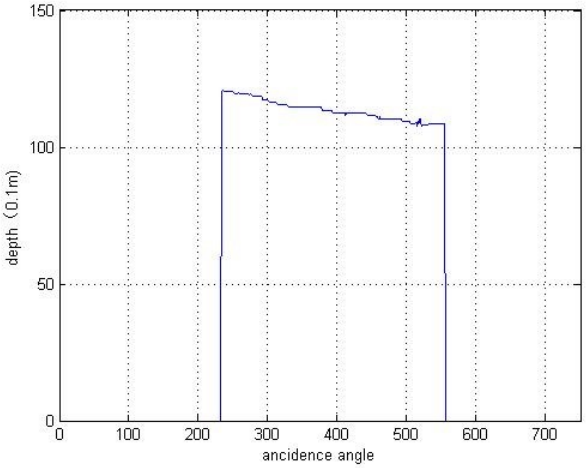

(b)Bottom-detection result with algorithm based on echo energy gradient

Fig. 7 comparison of algorithm results

We can see that This algorithm improves the defect of the original amplitude method, and has an excellent inhibition effect on the sidelobe interference.

C) Real shallow water

Echograms in fig. 8 are from the Reson SeaBat7125 Teledyne, carried out in the XuTai in January 2013. They display dense herring schools located closed to the seabed. The SeaBat was configured to, with incidence angle ranging from -50 to 50 and 3-dB beam widths ranging from 10 in the outer beams to 5 in the vertical beam. Because of the strong backscattering of the schools, amplitude-thresholding methods were unable to detect the bottom below the terrain.

Bottom-detection results using traditional amplitude method are illustrated in Fig. 9.

For smaller incidence angles, the maximum-amplitude method was as satisfactory as algorithm based on energy gradient.

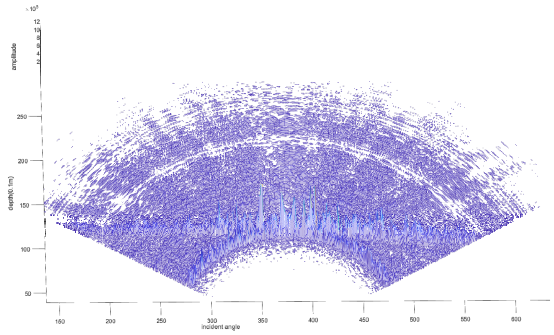

Fig. 8 A frame in echogram collected in the lake of lotus, XuYi

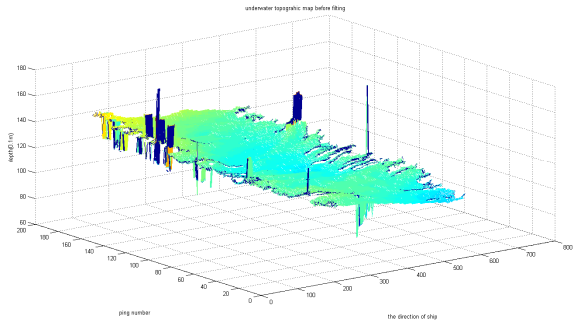

Fig. 9 Bottom-detection results using traditional amplitude method

It was noted, however, that the echo amplitude from side lobe interference was sometimes greater than that from the bottom. Thus, errors remained in the estimated bottom line. Although there is no ground truth data, we can intuitively see the differences between the algorithms through the modeling results.

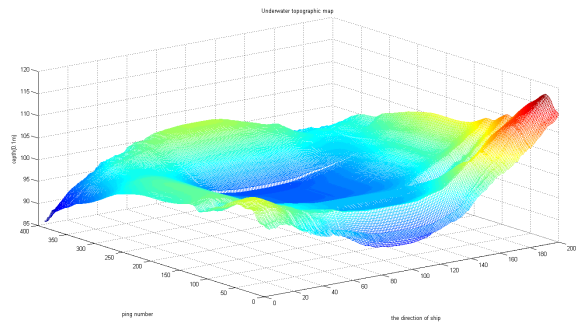

Fig. 10 Bottom-detection results using method proposed this paper

The algorithm based on energy gradient was applied to each bottom-line detection independently, i.e. only the spatial continuity between two consecutive pings in the same beam was considered. Results are plotted in Fig.10, proving that spikes have been removed efficiently.

CONCLUSIONS

New methods were investigated to improve bottom detection. In each beam, bottom detection can be performed by location the maximum of the amplitude for gradient image. Applying the new methods to the processing of echograms yielded satisfactory results. The errors caused by sidelobe interference can be effectively removed. However, such a detector still suffers from high variability and at times false bottom detections, especially at greater incidence angles and in deep water.

A state-space model for the seabed has been proposed, combined with an efficient Kalman-filter method, which efficiently stabilizes the detection. Applications to both simulation data and real data revealed that the algorithm can remove false detections caused by the presence of fish or other disturbance closed to the seabed.

Satisfactory results were achieved with a simulation data which made by Matlab and a real data collected by Seabat7125. When in a very irregular ground, this algorithm is poorly adapted to reality while bottom prediction by the state-space model and raw echo-based detection can lead to contradictory information.

REFERENCES

[1] Given. ROV Technology Trends And Forecast[C]// Oceans. IEEE, 1983.

[2] Sheikbahae M, Said A A, Stryland E W V. High-sensitivity, single-beam n2 measurements[J]. Optics Letters, 1989, 14(17):955.

[3] Colbo K, Ross T, Brown C, et al. A review of oceanographic applications of water column data from multibeam echosounders[J]. Estuarine, Coastal and Shelf Science, 2014, 145:41-56.

[4] Stepanova L, Ramazanov I, Kanifadin K. Estimation of time-of-arrival errors of acoustic-emission signals by the threshold method[J]. Russian Journal of Nondestructive Testing, 2009, 45(4):273-279.

[5] Kraeutner P, Brumley B, Guo H, et al. Rethinking Forward-Looking Sonar for AUV's: Combining Horizontal Beamforming with Vertical Angle-of-Arrival Estimation[C]// Oceans. IEEE, 2008.

[6] Bourguignon S, Berger L, Scalabrin C, et al. Methodological developments for improved bottom detection with the ME70 multibeam echosounder[J]. ICES Journal of Marine Science, 2009, 66(6):1015-1022.

[7] Lurton X. An Introduction to Underwater Acoustics[J]. Journal of the Acoustical Society of America, 2010, 115(115):443-443.

[8] Ona, E. Acoustic sampling and signal processing near the seabed: the deadzone revisited[J]. ICES Journal of Marine Science, 1996, 53(4):677-690.

[9] Maclennan D N, Copland P J, Armstrong E, et al. Experiments on the discrimination of fish and seabed echoes[J]. Ices Journal of Marine Science, 2004, 61(2):201-210.

[10] Zhang C, Wang H, Qiu Y. Sidelobe reduction of Acousto-optic tunable filter by double-filtering[J]. Proceedings of SPIE - The International Society for Optical Engineering, 2010, 7656.

[11] Caiti A, Bergem O, Dybedal J. Parametric sonars for seafloor characterization[J]. Measurement Science & Technology, 1999, 10(12):1105---11151115.

[12] Berger L, Poncelet C, Trenkel V M. A method for reducing uncertainty in estimates of fish-school frequency response using data from multifrequency and multibeam echosounders[J]. ICES Journal of Marine Science, 2009, 66(6):1155-1161.